Akita J Med **39** : 81–87, 2012

AGE-RELATED CHANGES IN ELECTROPHYSIOLOGICAL PROPERTIES IN CBA/N MICE UTRICULAR TYPE II HAIR CELLS

Kou Koizumi[1)], Eigo Omi[1)], Nakarin Angunsri[1)], Kohei Honda[1)], Kyoichi Ono[2)] and Kazuo Ishikawa[1)]

(received 20 December 2012, accepted 28 December 2012)

[1)]Department of Otorhinolaryngology, Head and Neck Surgery, Akita University Graduate School of Medicine, Akita, Japan
[2)]Department of Cell Physiology, Akita University Graduate School of Medicine, Akita, Japan

Abstract

Objective This study investigated vestibular functional declination with age, leading to age-related deterioration of balance function. It has been shown that the impaired vestibular function is derived from structural and/or functional degeneration of vestibular hair cells.

Methods We quantitatively analyzed the number of hair cells in the utricle of CBA/N mice at 2 different ages (5 weeks old and 26 weeks old) using immunohistochemistry. In addition, electrophysiological properties of type II hair cells were evaluated by the patch clamp method.

Results We found a significant difference in the number of hair cells between the two groups, i.e., the number of hair cells was significantly less in the adult group than in the young group. Electrophysiological experiments revealed that the current density of the delayed rectifier K^+ current was significantly lower in adult mice than in young mice, with little change in activation kinetics.

Conclusions These findings suggest that not only hair cell loss but also alterations in hair cell functions, resulting from aging, is involved in balance dysfunction.

Key words : vestibular organ, utricle, hair cell, voltage-gated conductance, inner-ear aging

Introduction

It is well known that balance function deteriorates with age. A number of studies have made attempts to characterize functional aspects of age-related balance problems. Although there is a marked variation in the results as a function of test paradigm, there is a general consensus that the decline of vestibular function underlies age-related balance problems. The vestibular system of the inner ear contains the otolith organs (utricle and saccule), which sense linear acceleration, and the semicircular canals, which detect angular acceleration. Two different types of vestibular hair cells, type I and type II, can be distinguished in these vestibular end-organs. These cells are classified according to the form of synaptic terminal made by afferent nerve fibers, and morphological characteristics. Type I cells are globular or flask-shaped and surrounded by calyceal afferent terminals, while type II cells are cylindrical and innervated by multiple afferent boutons[1,2)]. These two cell types also differ electrophysiologically, i.e., type I but not type II hair cells have a delayed rectifier conductance called g_{KL}[1,3–5)]. g_{KL} is substantially activated at the resting potential and represents a signature conductance in type I hair cells[1,2)]. On the other hand, a delayed rectifier, g_{DR} develops in type II hair cells postnatally[6)]. Although postnatal differentiation of hair cells has been well investigated[1)], little is known regarding age-related changes in

Correspondence : Kou Koizumi
Department of Otorhinolaryngology, Head and Neck Surgery, Akita University Graduate School of Medicine, 1-1-1 Hondo, Akita 010-8543, Japan
Tel : 81-18-884-6171
Fax : 81-18-836-2622
E-mail : koukoizumi@gmail.com

functional properties of hair cells.

It has been a common assertion that loss or degeneration of hair cells occurs during the aging process[7-9]. In fact, not only cochlear but also vestibular hair cells are involved in the sensory hearing loss or imbalance problems of aged people[10,11]. In addition, it has been reported that mouse cochlear hair cells are reduced and the threshold of compound action potential (CAP) is elevated during aging[12]. On the other hand, it has been shown that no significant loss of hair cells occurred in aged gerbil crista ampullaris[13] or in human utricular macula[14]. Thus, the evidence for a decrease in human vestibular hair cells during aging remains controversial.

In addition to changes in the number of vestibular hair cells, other morphological and functional changes could also contribute to balance problems among the elderly. However, little is known regarding aging-related changes in the functional properties of vestibular hair cells from previous studies, particularly the electrophysiological characteristics of hair cells during the aging process. In the present study, we have compared the electrophysiological properties of vestibular type II hair cells in two groups of CBA/N mice that are different in age by the patch clamp method, in order to characterize age-related changes in hair cell function. In addition, the numbers of vestibular hair cells in these groups were quantitatively analyzed by immunohistochemistry.

Materials and Methods

Animals

These studies used young (5 weeks) and adult (26 weeks) male CBA/N mice (Japan SLC Inc., Hamamatsu, Japan). All mice were bred under controlled conditions of temperature (22±0.5°C), humidity (50±10%) and lighting (12 h : 12 h light : dark cycle, light time began at 7 : 00 am), and were fed with a normal diet at the Institute of Laboratory Animals, Graduate School of Medicine, Akita University, Japan. Experimental protocols used in this study were approved by the Animal Ethics Committee of the Akita University School of Medicine in Japan, and complied with the US National Institutes of Health Guidelines for the Care and Use of Laboratory Animals.

Isolation of hair cells

Mice were deeply anesthetized with pentobarbital sodium (50-100 mg/kg ip) and decapitated. The temporal bones were rapidly dissected out and placed in a high-Ca^{2+} L-15 medium (see below). The utricles were excised and immersed in the low-Ca^{2+} L-15 medium containing papain (Wako, Osaka, Japan ; 500 μg/ml) and L-cysteine (Wako ; 300 μg/ml) for 40-50 min at 37°C, following which they were incubated in low-Ca^{2+} L-15 containing bovine serum albumin (Wako ; 500 μg/ml) for 10 min at room temperature (22-25°C). Utricles were then brushed gently with a fine probe. The dissociated hair cells were allowed to settle onto the glass floor of the recording chamber. All utricles were used within 5 h after isolation. The dissociated cells were viewed at ×600 with an inverted microscope (Nikon ECLIPSE TE2000-U, Tokyo, Japan). Type I and II cells were usually discriminated by their morphology, i.e, type I cells are globular or flask-shaped whereas type II cells are cylindrical. In addition, we used the morphometric criteria reported previously by Ricch *et al.*[15]. Namely, hair cells that satisfied the ratios of neck width to cuticular plate width (>0.72) and neck width to cell body width (>0.58) were identified as type II cells and used for electrophysiological experiments. The recording chamber was continuously perfused with high-Ca^{2+} L-15 medium at a rate of 1 ml/min.

Solutions

The external solution used for cell isolation and electrophysiological experiments was prepared from Leibovitz's L-15 medium (Sigma, St. Louis, MO, USA) additionally buffered with 10 mM HEPES. The high-Ca^{2+} L-15 medium was prepared by adding 2 mM $CaCl_2$ to the L-15 medium. The high-Ca^{2+} L-15 medium contained (in mM) 139 Na^+, 5.8 K^+, 3.3 Ca^{2+}, 1.8 Mg^{2+}, 147 Cl^-, 0.8 SO_4^{2-}, 0.8 HPO_4^{2-}, plus amino acids and vitamins. For the enzymatic and mechanical dissociation steps, we added 1.2 mM EGTA to reduce Ca^{2+} to 100 μM (low-Ca^{2+} L-15 medium). Both solutions were adjusted to pH 7.4 with NaOH and had an osmolality of 315-325 mmol/kg. The standard bath solution was high-Ca^{2+} L-15 medium. The pipette solution contained (in mM) : 140 KCl, 0.1

$CaCl_2$, 3.5 $MgCl_2$, 2.5 Na_2ATP, 5 EGTA, 5 HEPES. The pH was adjusted to 7.4 with KOH.

Electrophysiology

All recordings were done at room temperature (23～25°C). The whole-cell patch clamp method was used for recording membrane potentials and currents (Axopatch 200B, Molecular Devices, Sunnyvale, California, USA). An agar-Tyrode-Ag-AgCl bridge was used as an indifferent electrode. Borosilicate capillaries (Model 1.5 G, Narishige, Tokyo, Japan) were pulled and heat-polished to obtain pipette resistance of between 3 and 8 MΩ in our standard bath and pipette solutions. The current signal was filtered by a low pass Bessel filter with a cut-off frequency of 1 kHz, and digitized at 2 kHz using a Digidata 1440A A/D converter (Molecular Devices, Sunnyvale, California, USA) and stored on a computer for later analysis using pCLAMP version 10.0 software (Molecular Devices, Sunnyvale, California, USA). The cell membrane capacitance (C_m) was determined by applying a 30-ms hyperpolarizing voltage-clamp step from a holding potential of −40 mV to −50 mV and integrating the area under the capacitive transient.

Data were obtained from 5-week-old (n=14 from eight ears) and 26-week-old mice (n=14 from seven ears). Results are expressed as mean±SE. Statistical significance was determined using Student's t-test. A p value of <0.005 was considered statistically significant.

Cell counting by immunohistochemistry

Mice were deeply anesthetized with pentobarbital sodium and decapitated. The temporal bones were dissected out and the utricles were excised from the surrounding tissue in 0.1 M phosphate-buffered saline, pH 7.4. The otoconial membranes were gently removed with a fine needle. Explants of utricle sensory epithelia were placed intact on cover glass (Iwaki, Tokyo, Japan) and maintained in 24-well culture plates (Sumitomo Bakelite Co., Tokyo, Japan) in 4% PFA for 15 min. After fixation with 4% PFA, specimens were incubated with Alexa-Fluor Rhodamine-phalloidin (Invitrogen, Eugene, OR, USA) to label F-actin, and then viewed with a FV10i laser-scanning confocal microscope (OLYMPUS Inc.).

We observed whole images of utricles and classified them as striola regions and extrastriola regions. Firstly, we identified and marked the reversal line, the point at which kinocilia have opposite orientations, in a high magnification image. It is generally accepted that the striola corresponds to the central region of low hair cell density and to the band of calretinin-positive calyces[16,17]. In the present study, we designated the striola as low hair cell density area which lies medial to the reversal line (dotted area in Fig. 2a), as described by Li *et al.*[16]. Also, the localization of the striola was confirmed by the morphometric feature of the otolithic organs described by Desai *et al.*[17]. In both striola and extrastriola regions, square areas of 50×50 μm were isolated up. Hair cell numbers in each frame were counted, and the average of each region was used as the representative data for a specimen.

Data were obtained from 5-week-old mice (n=25 from eight ears) and 26-week-old mice (n=25 from eight ears). Results are expressed as mean±SE. Statistical significance was determined using Student's t-test. A p-value of <0.005 was considered statistically significant.

Results

Electrophysiological activation of type II hair cells

We firstly identified type II hair cells morphologically by observation under the light microscope (see Method). Type I and II cells may also be classified electrophysiologically. Type I hair cells have a delayed rectifier conductance called g_{KL}[1,3-5]. g_{KL} is substantially activated at the resting potential, and most hair cells without g_{KL} are type II cells[1,4,5,18]. Figures 1a and 1b show representative records of whole-cell currents obtained by standard voltage protocols in isolated type II hair cells of 5-week-old (a) and 26-week-old mice (b). In response to a 300-ms depolarizing pulse from −115 mV to various potentials, a time-dependent outward current was developed with increasing depolarization. The outward current decayed gradually during the depolarizing pulses and was reactivated upon repolarization to −45 mV. The configuration of the outward current was essentially the same as the g_{DR} reported in type II hair cells, and little or no g_{KL}-like current was observed in these cells. Thus, we were able to confirm that the hair cells we used in the

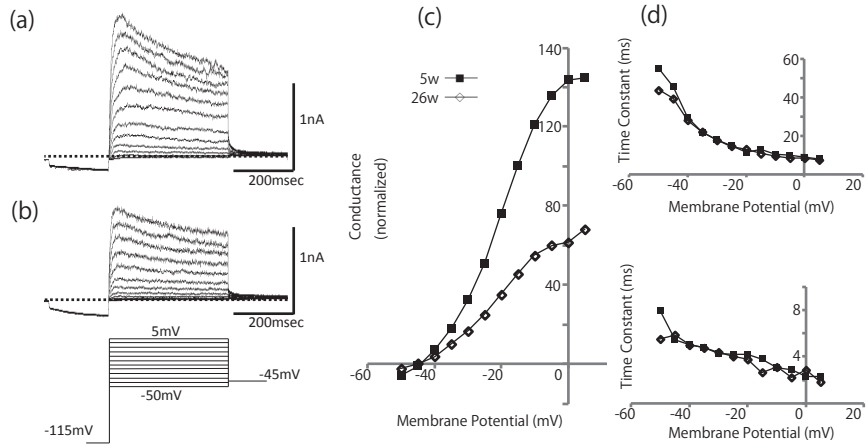

Fig. 1. G_{DR} in CBA/N mouse utricular hair cells. (a,b) : Families of current traces from a cell with g_{DR} (a, post natal 5-weeks ; b, post natal 26-weeks) in response to voltage steps from $V_H = -115$ mV. Data points between 0 msec and the peak of each outward current trace were fitted with Boltzmann functions and then extrapolated in time, as shown. In (a) and (b), the sigmoidally activating current positive to −50 mV is through g_{DR}. (c) : Activation curves are from the mean of 14 data points. Tail current at 26 weeks postnatal is clearly less than that of 5 weeks. Tail currents were fitted with double-exponential functions. On average, *Imax*, $V_{0.5}$ and S were 0.31±0.06 nS, −20.71±0.78 mV and 7.83±0.58 mV (n=14), respectively for 5-week-old mice, and 0.23±0.04 nS, −23.48±1.53 mV and 9.22±0.83 mV (n=14) for 26-week-old mice. (d) : Voltage dependence of activation time constants. Time constants were obtained by fitting activating currents with a sum of two exponential functions and are shown on separate ordinates for clarity : τ_1, top ; τ_2, bottom. Each of the time constants for g_{DR} is from the mean of fits to the current traces.

present study were mostly type II, not type I, cells.

The current density measured by the maximum conductance was significantly smaller in the 26-week-old group than the 5-week-old group. The tail current amplitude was measured, normalized in reference to cell capacitance, and plotted against the test potentials (Fig. 1c). The activation property was analyzed by applying the least squares method to the tail current amplitude fitted with a Boltzmann function,

$$I = I_{max} / [1 + \exp \{(V_m - V_{0.5}) / S\}],$$

where, *Imax*, $V_{0.5}$ and S indicate the maximal amplitude, the voltage showing half-activation and the slope factor, respectively (Fig. 1c). On average, *Imax*, $V_{0.5}$ and S were 0.31±0.06 nS, −20.71±0.78 mV and 7.83±0.58 mV (n=14), respectively for 5-week-old mice, and 0.23±0.04 nS, −23.48±1.53 mV and 9.22±0.83 mV (n=14) for 26-week-old mice. As a result, the maximum current density of g_{DR} was significantly smaller in the 26-week-old group than the 5-week-old group (p<0.005) with little difference in $V_{0.5}$ and the slope factor. This finding indicates that the current density of g_{DR} decreased with aging without affecting the kinetics. This view was confirmed by analyzing the time course of inactivation of g_{DR} at various test potentials. The time course of inactivation was fitted with a sum of two exponential functions, and the time constants of slow (Fig. 1d top) and fast components (Fig. 1d bottom) were plotted against the membrane potentials. No significant difference was detected for either component.

Hair cell counts

Fig. 2a shows the surface view of the mouse utricle. The striola is outlined by the broken line. We designated the reversal line of the kinocilia based on high magnification views of the utricle, and a representative image for 26-week mice is shown in Fig. 2b. Fig. 2c shows the average number of hair cells. The number of hair cells is significantly less in the 26-week-old group than the

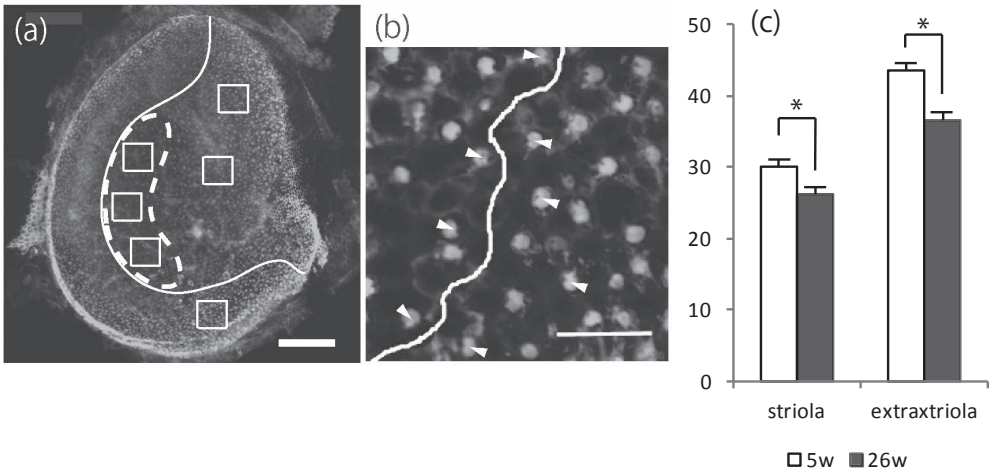

Fig. 2. The surface images of the utricle stained with rhodamine-phalloidin. (a) : A whole image of the utricle. The reversal line of kinocilia is shown by a curved solid line in the utricle. The striola region is enclosed with broken line. We designated squares whose size are 50 μm×50 μm in the striola and extrastriola regions. Scale bar represents 100 μm. (b) : High magnification view of the striola region of a 26-week-old mouse. A curved line represents the line of the polarity reversal. Arrowheads indicate the gap in phalloidin staining that marks the kinocilium and thus hair cell polarity. Scale bar represents 20 μm. (c) : The number of hair cells in each square was counted and quantitative analyses carried out. In each region, the numbers of hair cells are significantly different ($p<0.005$). Hair cells in 26-week-old mice are fewer than in 5-week-old mice. Data are expressed as mean±SE.

5-week-old group. The averages counted between the two groups were 30.2±1.03 (5-week-old group) and 26.2 ±0.90 (26-week-old group) at the striola region, and 43.7 ±1.01 (5-week-old group) and at 36.6±0.83 (26-week-old group) at the extrastriola region. In both regions, the numbers of hair cell were significantly different ($p<0.005$).

This result shows that there is a statistically-significant correlation between age and hair cell count (Fig. 2c). We observed that hair cells begin to scatter and become depleted upon growing older. However, there were no statistically-significant correlations between the two regions in either age group and we did not find any deformity or distortion of the cilia of hair cells in either group.

Discussion

Decline in electrophysiological function in type II hair cells

The present study demonstrates that the current density of g_{DR} is significantly less in 26-week-old mice than in 5-week-old mice, with little change in the kinetics. This finding may indicate that the expression of the g_{DR} channel in the cell membrane decreases with aging. It has been reported that g_{KL} in type I cells is first observed at the fourth day after birth and its current density increases to mature levels at the fourth postnatal week, whereas the magnitude and activation of outward K^+ currents in type II cells do not change during the same postnatal period[19]. It should be noted, however, that that study focused on postnatal development, not on the aging process. Regarding cochlear aging, a previous report showed that the functional decline begins at approximately 17-19 months[12]. Although vestibular decline will not necessarily be the same as for the cochlea, the present results may indicate that the decrease in the number of K^+ channels associated with g_{DR} is involved in vestibular decline during the aging process.

In this study, we compared 5- and 26-week-old mice, which may not represent age-related functional differences in hair cells. But, in view of the human inner ear dysfunction that often occurs in people not fully in old

age, it is probable that potential dysfunction exists in the adult inner ear. We propose that the present data supports the view that functional decline of hair cells occurs in adult mice. Furthermore, the significant difference observed between 5- and 26-week-old mice promises more functional decline in aged mice. Moreover, not only type II cells but also type I, which are "super-differentiated" type II cells[1], may degenerate with aging. It will be meaningful to investigate the course of vestibular degeneration with aging by neurophysiological examination.

Loss of utricular hair cells during aging

In the 26-week-old group, the numbers of utricular hair cells in the striola and extrastriola regions were significantly less than the 5-week-old group. In mouse cochlea, hair cells decrease with aging[12]. Therefore, we morphologically examined the utricles to see whether vestibular hair cell decrease is accompanied by electrophysiological change.

It has been reported that a decrease in hair cells does not occur with aging[13]. However, our current results agree with other previous studies that indicate degeneration of hair cells with aging[20,21]. In most of the studies in aged human temporal bone, statistically-significant amounts of hair cell loss were shown. Due to the longer life span of humans compared to rodents, long term asymptomatic underlying diseases such as vascular sclerosis and increased levels of reactive oxidative species (ROS) in essentially all tissues during aging, and DNA of mitochondria perished as a consequence of ROS action, also accumulate progressively, causing degeneration of hair cells[22,23]. In addition, it has been observed that age-related changes in cell loss and degeneration over time can only be seen in type I, but not in type II, hair cells and supporting cells as well as the efferent and afferent nerve endings in the vestibular epithelium[24,25].

The cell counting method used in this study did not distinguish type I and type II cells. However, it is important that a significant reduction was observed in the entire number of hair cells. In future studies, cell count will need to be divided into types I and II, with a use of a marker for type II hair cells in mice such as calretinin.

As for functional decline, it is expected that the number of hair cells will decrease in other inner ear organs to a greater degree in aged mice.

Acknowlegments

For expert histological and technical assistance, Dr. Eiko Ito is kindly thanked. The animals were treated in the most gentle and professional way by Kuniko Furuki. Dr. Yohei Kawasaki is warmly thanked for the interesting discussions and critical comments and suggestions on the manuscript.

References

1) Rüsch, A., Lysakowski, A. and Eatock, R.A. (1998) Postnatal development of type I and type II hair cells in the mouse utricle : Acquisition of voltage-gated conductances and differentiated morphology. *J. Neurosci.*, **18**, 7487-7501.
2) Brichta, A.M. and Goldberg, J.M. (2000) Morphological Identification of Physiologically Characterized Afferents Innervating the Turtle Posterior Crista. *J. Neurophysiol.*, **83**, 1202-1223.
3) Correia, M.J. and Lang, D.G. (1990) An electrophysiological comparison of solitary type I and type II vestibular hair cells. *Neurosci. Lett.*, **116**, 106-111.
4) Eatock, R.A., Chen, W.Y. and Saeki, M. (1994) Potassium currents in mammalian vestibular hair cells. *Sens. Syst.*, **8**, 21-28.
5) Ricci, A.J., Rennie, K.J. and Correia, M.J. (1996) The delayed rectifier, IKI, is the major conductance in type I vestibular hair cells across vestibular end organs. *Pflügers. Arch.*, **432**, 34-42.
6) Géléoc, G.S., Risner, J.R. and Holt, J.R. (2004) Developmental acquisition of voltage-dependent conductances and sensory signaling in hair cells of the embryonic mouse inner ear. *J. Neurosci.*, **24**, 1148-1159.
7) Engstrom, H., Bergstrom, B. and Rosenhall, U. (1974) Vestibular sensory epithelia. *Arch. Otolaryngol.*, **100**, 411-418.
8) Richter, E. (1980) Quantitative study of human Scarpa's ganglion and vestibular sensory epithelia. *Acta Otolaryngol.*, **90**, 199-208.

9) Merchant, S.N., Velázquez-Villaseñor, L., Tsuji, K., Glynn, R.J., Wall, C. 3rd. and Rauch, S.D. (2000) Temporal bone studies of the human peripheral vestibular system. Normative vestibular hair cell data. *Ann. Otol. Rhinol. Laryngol. Suppl.*, **181**, 3-13.
10) Peterka, R.J. and Black, F.O. (1991) Age-related changes in human posture control : motor coordination tests. *J. Vestib. Res.*, **1**, 87-96.
11) Paige, G.D. (1994) Senescence of human visual-vestibular interanctions : smooth pursuit, optokinetic, and vestibular control of eye movements with aging. *Exp. Brain Res.*, **98**, 355-372.
12) Ohlemiller, K.K., Dahl, A.R. and Gagnon, P.M. (2010) Divergent aging characteristics in CBA/J and CBA/CaJ mouse cochleae. *J. Assoc. Res. Otolaryngol.*, **11**, 605-623.
13) Kevetter, G.A., Zimmerman, C.L. and Leonard, R.B. (2005) Hair cell numbers do not decrease in the crista ampullaris of geriatric gerbils. *J. Neurosci.*, **80**, 279-285.
14) Gopen, Q., Lopez, I., Ishiyama, G., Baloh, R.W. and Ishiyama, A. (2003) Unbiased stereological type I and type II hair cell counts in human utricular macula. *Laryngoscope*, **113**, 1132-1138.
15) Ricch, A.J., Rennie, K.J., Cochran, S.L., Kevetter, G.A. and Correia, M.J. (1997) Vestibular type I and type II hair cells. 1 : morphometric identification in the pigeon and gerbil. *J. Vestib. Res.*, **7**, 393-406.
16) Li, A., Xue, J. and Peterson, E.H. (2008) Architecture of the mouse utricle : macular organization and hair bundle heights. *J. Neurophysiol.*, **99**, 718-733.
17) Desai, S.S., Zeh, C. and Lysakowski, A. (2005) Comparative morphology of rodent vestibular periphery. I. Saccular and utricular maculae. *J. Neurophysiol.*, **93**, 251-266.
18) Rüsch, A. and Eatock, R.A. (1996) A delayed rectifier conductance in type I hair cells of the mouse utricle. *J. Neurophysiol.*, **76**, 995-1004.
19) Hurley, K.M., Gaboyard, S., Zhong, M., *et al.* (2006) M-like K^+ currents in type I hair cells and calyx afferent endings of the developing rat utricle. *J. Neurosci.*, **40**, 10253-10269.
20) Rauch, S.D., Velazquez-Villaseñor, L., Dimitri, P.S. and Merchant, S.N. (2001) Decreasing hair cell counts in aging humans. *Ann. N. Y. Acad. Sci.*, **942**, 220-227.
21) Walther, L.E. and Westhofen, M. (2007) Presbyvertigo-aging of otoconia and vestibular sensory cells. *J. Vestib. Res.*, **17**, 89-92.
22) Lee, C.K., Weindruch, R. and Prolla, T.A. (2000) Gene-expression profile of the ageing brain in mice. *Nat. Genet.*, **25**, 294-297.
23) Sohal, R.S. and Weindruch, R. (1996) Oxidant stress, caloric restriction, and aging. *Science*, **273**, 59-63.
24) Sobin, A. and Wersäll, J. (1983) A morphological study on vestibular sensory epithelia in a strain of the waltzing guinea pig. *Acta Otolaryngol. Suppl.*, **396**, 1-32.
25) Severinsen, S.A., Raarup, M.K., Ulfendahl, M., Wogensen, L., Nyengaard, J.R. and Kirkegaard, M. (2008) Type I hair cell degeneration in the utricular macula of the waltzing guinea pig. *Hear Res.*, **236**, 33-41.